Journal of Volcanology and Geothermal Research xxx (2016) xxx–xxx

Contents lists available at ScienceDirect

Journal of Volcanology and Geothermal Research

journal homepage: www.elsevier.com/locate/jvolgeores

Sensitivity analysis of a one-dimensional model of a volcanic plume with particle fallout and collapse behavior

S. Pouget, M. Bursik *, P. Singla, T. Singh

University at Buffalo, Buffalo, NY, USA

ARTICLE INFO

Article history:
Received 3 October 2015
Received in revised form 17 February 2016
Accepted 19 February 2016
Available online xxxx

Keywords:
Volcanic plume
Source conditions
Entrainment
Uncertainty
Sensitivity
Pearson coefficient
Distance correlation
Linear coefficient
Global sensitivity
Main effect
Total effect

ABSTRACT

We run a volcanic plume model with uncertain boundary conditions and entrainment related model parameters. Output variables tested for their sensitivity to the inputs are total rise height, and mass flux of particles into the umbrella cloud or downwind plume. Boundary or source conditions are vent radius, initial velocity, grain size mean and grain size standard deviation. Model parameters are entrainment rate, α, wind entrainment rate, β, and wind speed.

Five sensitivity metrics were considered. Three of these are calculated for each given point in the input parameter space, by perturbing the input variable around fixed points. Two global sensitivity measures quantify the impact on the output of the input over its entire uncertain domain.

We find that vent radius and initial speed have a much more profound effect on both outputs than does total grain size distribution. Plume rise height and particle mass flux are sensitive to the entrainment parameters, α and β, but these parameters are not of greater importance than the wind speed. This suggests that while efforts to better characterize entrainment parameters through laboratory experiments is important, similar efforts should be made to collect appropriate meteorological data for the region near the site of the eruption.

1. Introduction

One-dimensional, numerical eruption column or plume models (Costa et al., this volume) have found a use in estimation of the amount of ash emplaced into the atmosphere at an estimated plume height (e.g., Folch et al., 2008). The nature of the sensitivity of the output ash loading or plume height to the variables and parameters that are incorporated in a given plume model is however poorly known (Scollo et al., 2008; Degruyter and Bonadonna, 2012; Woodhouse et al., 2015, this volume). One expects, based on previous experience, that plume height and atmospheric loading should primarily be functions of grain size, vent radius, and plume velocity (Sparks et al., 1997).

The eruption plume model discussed in the present contribution was introduced by Bursik (2001). As part of a larger program of improvement and recasting, in the present contribution, it has been modified in a number of ways. These changes were precipitated by the work presented in Bursik et al. (2012) and Stefanescu et al. (2014). The changes to the original plume model are as follows. The model:

1. Has been modified to provide input to PUFF or HYSPLIT (Bursik et al., 2013).
2. Can use radiosonde or NWP data directly to get atmospheric parameters.
3. Can estimate atmosphere above the top of radiosonde or NWP data used as input.
4. Can be run in stochastic mode with uncertain inputs of volcanic boundary conditions as well as entrainment parameters and wind speed.
5. Can be run in inverse mode to estimate source parameters.
6. Can simulate collapse behavior, to allow fountain height to be recorded. In these cases, there is no injection of pyroclasts from the vent into the atmosphere.
7. Includes a refined model for plume rise height calculation.

Other changes to the model not included in the present version – to keep it as close to the model of Bursik (2001) as possible – are the following:

1. Modules for water have been added (Glaze and Baloga, 1996).
2. Double-precision and adaptive step-size now used.
3. Previously little-documented, optional, umbrella cloud and fallout modules (Bursik et al., 2009) are available.

The model was originally unnamed, but was later called BENT (Bursik et al., 2009). The present incarnation is called "puffin," to

* Corresponding author.

http://dx.doi.org/10.1016/j.jvolgeores.2016.02.018
0377-0273/

emphasize the fact that it can be used to provided input to PUFF or HYSPLIT (Bursik et al., 2013).

We concentrate herein on discussing results from running the model with uncertain boundary conditions and entrainment related parameters in a full sensitivity analysis. The output variables to be tested for their sensitivity to the inputs are total rise height, H_T, and mass flux of particles into the umbrella cloud or downwind plume, $\dot{m}_p|_{H_B}$, which are responsible for the atmospheric loading. First we introduce the current set of equations of motion, and then we introduce the methods and metrics to be used in the analysis. Finally, we present a consideration of the meaning of the results.

2. Model of plume motion

The deterministic plume model was presented previously (Bursik, 2001), and is an integral, one-dimensional model for plumes that entrain mass and momentum from the wind (Hewett et al., 1971; Wright, 1984). The model includes a spectrum of pyroclasts of different grain sizes and settling speeds that move at the same speed as the plume gases until falling out from the plume margins. Once falling they can be re-entrained. It is a trajectory model, and therefore well-suited for adaptation to and coordination with meteorological models and data. The following presentation follows that in (Bursik, 2001), but has been explicitly modified to highlight the variables and parameters that are now treated as stochastic.

2.1. Coordinate system

In the following analysis, the downwind distance is x, z is up, and s represents the distance along the plume axis from the vent. Theta, ϑ, is the inclination of the plume centerline to the horizon. The equations expressing the relationship between (x,z) and (s,ϑ) are then given by:

$$x = \int \cos\vartheta ds, \tag{1}$$

$$z = \int \sin\vartheta ds. \tag{2}$$

2.2. Equations of plume motion

In plumes that are significantly affected by the wind, the entrainment speed, U_ε, must be a function of wind speed, $V(\xi)$, now a stochastic variable given as a function of the unit random variable, ξ, as well as axial plume speed, U. A number of wind entrainment relationships have been investigated (see Table 2.1 in Wright, 1984, for an older summary). Reasonable correspondence between one such entrainment relation and experimental data has been obtained (Hewett et al., 1971):

$$U_\in = \alpha(\xi)|U - V(\xi)\cos\vartheta| + \beta(\xi)|V(\xi)\sin\vartheta|, \tag{3}$$

where $\alpha(\xi)$, the radial entrainment parameter and $\beta(\xi)$, the wind-entrainment parameter, are both now stochastic – but constant – parameters. Thus, we now have three stochastic *model parameters*: $V(\xi),\alpha(\xi),\beta(\xi)$. With this knowledge, henceforth the ξ will be dropped from the description of these variables. Eq. (3) assumes that the magnitude of the horizontal wind component is much larger than the vertical component. The practical meaning behind V, α and β being stochastic is that numerous, carefully selected values for these will be substituted into the equations of motion. Among other things, this will allow for exploration of the range of values for the entrainment parameters from the literature. Some of these different values may arise from near-vent phenomena, where plume density may be five times that of the ambient atmosphere (Sparks et al., 1997), and plume decompression occurs in the crater (Woods and Bower, 1995), or from a Richardson number dependence (Wang and Law, 2002; Kaminski and Tait, 2005).

For mass conservation (continuity) of the plume, we have:

$$\frac{d}{ds}\left(\pi b^2 \rho U\right) = 2\pi\rho_a b U_\epsilon + \sum_{i=1}^{N}\frac{dM_i}{ds}, \tag{4}$$

where b is the characteristic plume radius, ρ is the bulk plume density, ρ_a is the ambient atmospheric bulk density, and M_i represents the mass flux of pyroclasts of size fraction i within the plume. The first term on the right-hand side represents the gain in mass flux by entrainment of air, whereas the second term represents the loss of mass flux by fallout of pyroclasts.

The conservation of mass flux of particles for multiple grain size fractions, M_i, is given by (Ernst et al., 1996):

$$\frac{dM_i}{ds} = -\frac{\hat{p}w_s}{bU}M_i, \tag{5}$$

where $\hat{p}$ is a probability that an individual particle will fall from the plume and w_s is the settling speed of a particle in the given size class (in the current model, $i=1$ to 19 for pyroclasts between 10 and $-8\,\Phi$ at $1-\Phi$ intervals). The probability of fallout, $\hat{p}$, is a function of plume geometry and re-entrainment (Bursik, 2001), and should have an approximately constant value of ~0.23 with no re-entrainment, based on the geometry of plume margins in a quiescent atmosphere (Ernst et al., 1996). Because of the strong inflow towards the plume caused by entrainment, pyroclasts <~10 cm are, however, re-entrained at lower heights in a plume after falling from greater heights. Fitting a curve through experimental results for a vertical plume in a quiescent ambient Ernst et al. (1996), a reasonable, purely heuristic, form of the re-entrainment function, f, is:

$$f = 0.43\left(1 + \left[\frac{0.78}{F_0^{1/2}\mu_0^{-1/4}/w_{si}}\right]^6\right)^{-1}, \tag{6}$$

where F_0 is the specific thermal flux at the vent, $F_0 = b_0^2 U_0 C_{v\,0} T_0$, and μ_0 is the specific momentum flux at the vent, given by $\mu_0 = b_0^2 U_0^2$, and settling speeds of pyroclasts, $w_{s\,i}$ is calculated as a function of height, given atmospheric density and viscosity. With wind, Eq. (3) can be at best a poor approximation, as the pyroclasts on the downwind side would often not be re-entrained, given that the net horizontal wind speed can be away from the plume. However, at low wind speed, a zeroth-order assumption – made herein – is that the enhanced fallout on the downwind side is balanced by an enhanced re-entrainment on the upwind side.

The equation for conservation of axial momentum is:

$$\frac{d}{ds}\left(\pi b^2 \rho U^2\right) = \pi b^2 \Delta\rho g \sin\vartheta + V\cos\vartheta\frac{d}{ds}\left(\pi b^2 \rho U,\right), \tag{7}$$

where the first term on the right-hand side represents the change in momentum caused by the component of gravitational acceleration, $\Delta\rho g = (\rho_a - \rho)g$, in the axial direction, and the second term represents entrainment of momentum from wind. Note that this equation is modified from that in Bursik (2001), by taking out an explicit dependence on dM_i/ds, which because the effect of loss of pyroclasts on momentum flux is already counted in the second term on the RHS, resulted in a doubling of the effect of pyroclast fallout on plume dynamics. The conservation of the radial component of momentum is given by:

$$\left(\pi b^2 \rho U^2\right)\frac{d\vartheta}{ds} = \pi b^2 \Delta\rho g\cos\vartheta - V\sin\vartheta\frac{d}{ds}\left(\pi b^2 \rho U\right), \tag{8}$$

Please cite this article as: Pouget, S., et al., Sensitivity analysis of a one-dimensional model of a volcanic plume with particle fallout and collapse behavior, J. Volcanol. Geotherm. Res. (2016), http://dx.doi.org/10.1016/j.jvolgeores.2016.02.018

where the left-hand side represents the change in ϑ caused by the entrainment of momentum at an angle to the plume axis by both gravity (first term on right-hand side) and wind (second term). Note that the small-angle approximation is made for $d\vartheta$. The conservation of specific enthalpy is given by:

$$\frac{d}{ds}\left(\pi b^2 \rho U C_v T\right) = 2\pi b U_\epsilon \rho_a C_a T_a - \pi b^2 \rho U g \sin\vartheta + C_p T \sum_{i=1}^{N} \frac{dM_i}{ds}. \quad (9)$$

The first term on the right-hand side is the energy added by the entrainment of air, the second term is the change in thermal energy by conversion to/from gravitational potential energy, and the third term is the loss of heat by sedimentation of pyroclasts. C_v is the bulk heat capacity (all at constant pressure) of the material in the plume, T is its temperature, C_a and T_a are the heat capacity and temperature respectively of the air, and C_p is the heat capacity of the pyroclasts. The material in the plume is assumed initially to contain pyroclasts and water vapor, which is diluted by entrainment of air to concentration, $n = n(s)$, as a fraction of gas in the plume. All bulk properties are calculated as the weighted mean of the values for the separate phases, following Woods and Bursik (1991).

To calculate the concentration of pyroclasts at any radial position within the plume, we rely on the observation, frequently corroborated in experiment, that the time-mean concentration of any passive tracer or particle fraction in a plume in a quiescent ambient has a Gaussian profile (Morton et al., 1956). Thus the concentration as a function of radial distance, $C_i(r)$, within a volcanic plume follows:

$$C_i(r) = \frac{M_i}{\pi b^2 U} \exp\left[-\frac{r^2}{b^2}\right]. \quad (10)$$

This may be a particularly poor assumption for bent-over or weak plumes in high-speed ambient fluids.

The steady equations of motion are subject to the boundary conditions at the vent, denoted by a null subscript:

$$\begin{aligned} U &= U_0(\xi) \\ b &= b_0(\xi) \\ T &= T_0 \\ n_w &= n_{w0} \\ Md_\Phi &= Md_{\Phi 0}(\xi) \\ \sigma_\Phi &= \sigma_{\Phi 0}(\xi). \end{aligned} \quad (11)$$

where n_w is the mass fraction of water in the plume, Md_Φ is the median grain size, in Φ units, and σ_Φ is the standard deviation of the grain size distribution. All the above, except n_w, are prognostic variables, solved for by a fourth-order Runge–Kutta routine with Eqs. (4) through (9). Time-mean radial concentration profiles are calculated with Eq. (10). Intrinsic plume material properties and n_w are diagnostic, updated at each time step according to mass-averaging relations discussed elsewhere (Woods and Bursik, 1991; Sparks et al., 1997). Thus, in total we will explore four stochastic *boundary or source conditions*, as well as three stochastic *model parameters* (Eq. (11)).

2.3. Atmosphere

The present version of the model can use theoretical atmospheric profiles to test ideal cases of wind speed or other parameters, but can also use as input radiosonde or numerical weather prediction (NWP) data. For the present exercise, radiosonde data were given (Costa et al., this volume. However, for the sensitivity analysis, we seek to test the effect of wind speed and to compare that with the effect of the entrainment parameters. For this reason, we have used a wind speed that is constant with height. For other atmospheric parameters, we use standard values for the ICAN atmosphere, following Bursik (2001).

2.4. Rise height and mass flux estimation

The sensitivity of two output variables of interest is of concern: the total rise height, H_T, and the mass flux of pyroclasts into the umbrella cloud, estimated as the mass flux of pyroclasts at the neutral buoyancy height, $\dot{m}_p|_{H_B}$. The neutral buoyancy height or level, H_B, is assumed to occur where $\rho = \rho_a$ and $d(\rho - \rho_a)/ds > 0$. Total rise height is found as $H_T = H_B + U_z|_{H_B}{}^2/2g$, i.e., the top is defined by the momentum overshoot of the neutral buoyancy height, assuming no entrainment above H_B.

3. Model sensitivity

The main purpose of the sensitivity analysis of the plume model is to identify the relative importance of the uncertain parameters and source variables in controlling the most critical output variables: rise height, H_T, and atmospheric mass loading, $D \times \dot{m}_p|_{H_B}$, where D is eruption duration, which is not a variable in a steady plume model. The uncertain variables of interest are divided into the two categories, *model parameters* and *boundary* or *source conditions*, and are given in Table 1. To study the sensitivity of the plume model output to the uncertain parameters and boundary values of the source variables, five metrics were considered. Three of these are calculated for each given point in the input parameter space.

3.1. Pearson coefficient

The Pearson correlation coefficient, ρ_{XY}, is a measure of the linear correlation (dependence) between two random variables, X and Y, and is widely used as a measure of the degree of linear dependence between them. It is defined as the covariance of the two variables divided by the product of their standard deviations:

$$\rho_{XY} = \frac{E[(X-\mu_X)(Y-\mu_Y)]}{\sigma_X \sigma_Y}, \quad (12)$$

where E denotes expectation, μ_X and μ_Y denote the mean of variables X and Y, respectively, over all numerical experiments, σ_X and σ_Y denote the standard deviation. These variables are defined as usual:

$$\mu_X = E[X], \mu_Y = E[Y], \sigma_X^2 = E\left[(X-\mu_X)^2\right], \sigma_Y^2 = E\left[(Y-\mu_Y)^2\right]. \quad (13)$$

Accordingly, ρ_{XY} lies between $+1$ and -1 where 1 is total positive correlation, 0 is no correlation, and -1 is total negative correlation.

3.2. Distance correlation

It is well known that the Pearson correlation coefficient can be zero even for dependent variables. This usually happens whenever there is a symmetry in the relation between two variables. To address this

Table 1
Stochastic model parameters and source conditions.

Model parameter	Value range	PDF
Entrainment parameter, α	0.05–0.2	Uniform
Wind entrainment parameter, β	0.05–1.0	Uniform
Wind speed, V, m/s	0–30	Uniform
Source condition	**Value range**	**PDF**
Vent radius, b_0, m	50–300	Uniform
Velocity at vent, U_0, m/s	50–300	Uniform
Median grain size, Md_Φ, Φ units	−5–5	Uniform
σ_Φ, Φ units	1–5	Uniform

Please cite this article as: Pouget, S., et al., Sensitivity analysis of a one-dimensional model of a volcanic plume with particle fallout and collapse behavior, J. Volcanol. Geotherm. Res. (2016), http://dx.doi.org/10.1016/j.jvolgeores.2016.02.018

particular deficiency of the Pearson coefficient, the distance correlation was introduced almost a decade ago (Székely et al., 2007). The distance correlation is zero if and only if the variables are statistically independent. It is derived from the distance variance, distance standard deviation and distance covariance, which substitute for the ordinary moments in the definition of the Pearson correlation coefficient.

To define the distance correlation, we start with the definition of pairwise distance. If (X_i, Y_i) with $i = 1, 2, \ldots, N$ denote N samples of random variables (X, Y), then all pairwise distances are defined as:

$$a_{ij} = |X_i - X_j|, b_{ij} = |Y_i - Y_j|, i, j = 1, 2, \ldots, N. \tag{14}$$

Now, the distance covariance is defined as:

$$d\sigma^2_{XY} = \frac{1}{N^2}\sum_{i,j=1}^{N} A_{ij}B_{ij}, \tag{15}$$

where A_{ij} and B_{ij} are defined as:

$$A_{ij} = a_{ij} - E[a_{i,}] - E[a_{,j}] + E[a], \tag{16}$$

where $E[a_{i,}]$ denotes the mean of ith row of the matrix a_{ij} whereas $E[a_{,j}]$ denotes the mean of the jth column of the matrix a_{ij}. $E[a]$ is the mean of the matrix a_{ij}. The notation is similar for the b_{ij} values. It should be noticed that all rows and all columns of both $A_{i,j}$ and $B_{i,j}$ sum to zero. Now, the distance correlation $(d\rho_{XY})$ is defined by replacing ordinary statistical moments with distance moments, i.e.,

$$d\rho_{XY} = \frac{d\sigma^2_{XY}}{d\sigma_X d\sigma_Y}, \tag{17}$$

where $d\sigma_X = (d\sigma_{XX})^{1/2}$ and $d\sigma_Y = (d\sigma_{YY})^{1/2}$. The distance correlation, $d\rho_{XY}$, replaces the usual covariances of ρ_{XY} with local covariances. Thus $y(x)$ could be any more complex function, such as one symmetric about the y-axis, yet would show positive correlation between X and Y. Moreover, unlike ρ_{XY}, $d\rho_{XY}$ lies between zero and unity.

3.3. Linear coefficient

The third metric corresponds to finding the best linear dependence between the variables X and Y over the whole uncertain domain. Spanos (1981) suggested the technique of statistical linearization, by which the variable Y, a given nonlinear function of the random variable, X, can be approximated as a linear function of X:

$$Y = mX + c, \tag{18}$$

where the unknown coefficients, m and c are computed by minimizing the following error index:

$$\begin{aligned} J &= \min_{m,c} \int (Y - mX - c)^2 p(X) dX = E\left[(Y - mX - c)^2\right], \\ m &= \frac{E[YX] - E[X]E[Y]}{E\left[X^2\right] - E[X]E[X]}, \\ c &= E[Y - mX] = \frac{E\left[X^2\right]E[Y] - E[XY]E[X]}{E\left[X^2\right] - E[X]E[X]}, \end{aligned} \tag{19}$$

and $p(X)$ is the pdf of X. The minimization process leads to the following closed-form expressions for the unknown coefficients:

$$m = E[YX], c = E[Y]. \tag{20}$$

It should be noted that m can be interpreted as the gradient of Y with respect to X over the whole uncertain space.

In addition to the three metrics discussed above, *Global Sensitivity* measures have been increasingly used in geophysical applications (Chu-Agor et al., 2011; van Griensven et al., 2006; Pappenberger et al., 2008; Scollo et al., 2008; Woodhouse et al., 2015). As opposed to traditional sensitivity measures, which are determined by perturbing the input variable around fixed points, global sensitivity analysis aims to quantify the impact on the output of the input over its entire uncertain domain. Two global sensitivity metrics are considered, namely: (1) Main Effect and (2) Total Effect, which are described as follows.

3.4. Main effect

Global sensitivity analysis permits the evaluation of the contributions of uncertain inputs $X = x$ in characterizing the uncertainty in the output $Y = y$. *Factor Prioritization* is an approach in which the goal is to rank the variables based on the fraction of the output variance that is reduced when a specific value is assigned to the input variable.

The uncertainty in the output is parameterized by the variance when the remaining uncertain input parameters are varied across their domain. The importance of a variable, i.e., the sensitivity of the output to its value, can be gauged by the reduction in the variance of the output when the uncertainty in that variable is eliminated. A specific value is assigned to the variable x_i and the mean of the output over the rest of the uncertain variables is calculated. This value is given by the conditional mean:

$$E_{\tilde{x}_i}(Y|x_i = x_i^*), \tag{21}$$

where $\tilde{x}_i$ is the vector x without the parameter x_i. Since the constant x_i^* is not known and can take values which span a range, the variance of the conditional mean is determined over all possible values of x_i and is given by the equation:

$$V_{x_i}\left(E_{\tilde{x}_i}(Y|x_i = x_i^*)\right). \tag{22}$$

This measure is called the *Main Effect* of x_i on y and the larger its value, the larger is its influence on the output, which implies that the output variable is highly sensitive to x_i. The sensitivity is quantified as:

$$S_{x_i} = \frac{V_{x_i}\left(E_{\tilde{x}_i}(Y|x_i = x_i^*)\right)}{V(Y)}, \tag{23}$$

which lies in the range of zero to one, and is often referred to in the literature as the *first-order effect* (Saltelli et al., 2004).

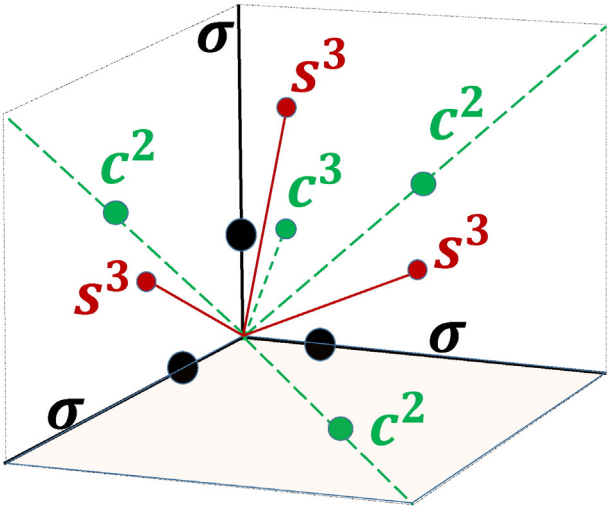

Fig. 1. Schematic of specially chosen axes according to CUT methodology in 3-D space. σ, principal axes. c^m, conjugate axes.

Please cite this article as: Pouget, S., et al., Sensitivity analysis of a one-dimensional model of a volcanic plume with particle fallout and collapse behavior, J. Volcanol. Geotherm. Res. (2016), http://dx.doi.org/10.1016/j.jvolgeores.2016.02.018

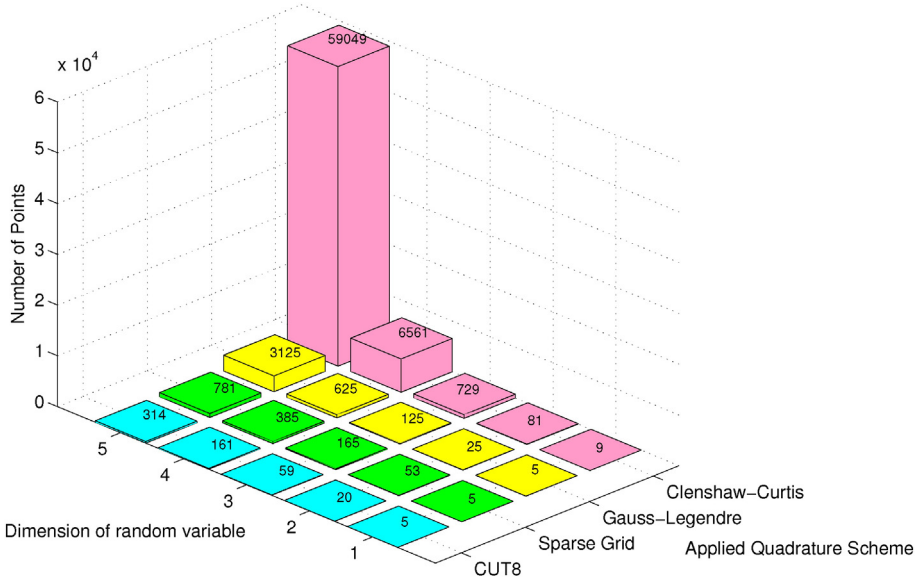

Fig. 2. Comparison of number of 8th order quadrature points required for different quadrature schemes, as a function of dimensionality (number) of random variables.

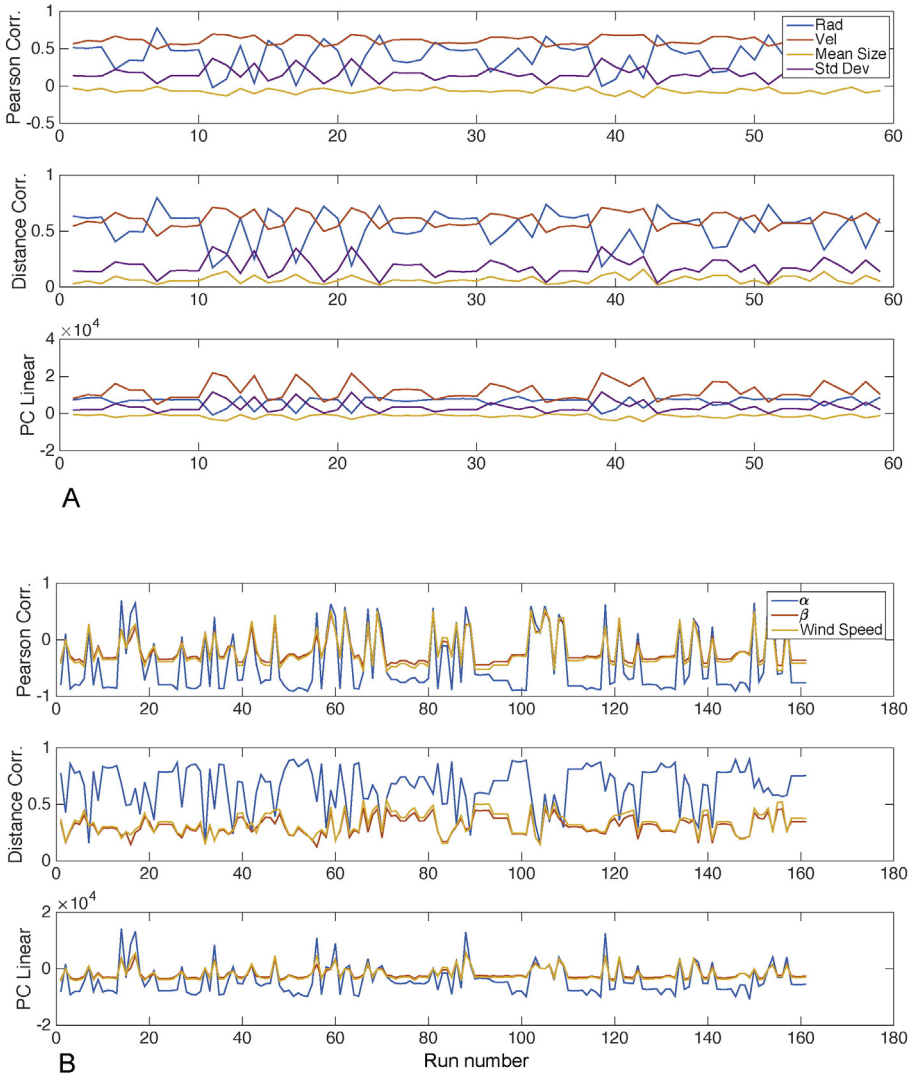

Fig. 3. Results of different sensitivity metrics for plume height, H_T. Each run number refers to computational run using different CUT point (set of values of variables being tested for sensitivity). A) Sensitivity as a function of source parameters. B) Sensitivity as a function of source conditions.

Please cite this article as: Pouget, S., et al., Sensitivity analysis of a one-dimensional model of a volcanic plume with particle fallout and collapse behavior, J. Volcanol. Geotherm. Res. (2016), http://dx.doi.org/10.1016/j.jvolgeores.2016.02.018

3.5. Total effect

A second measure to gauge the importance of the variable x_i over its range of uncertainty is given by the contribution to the variance of the output of x_i, including all effects resulting from its interactions with other uncertain variable of any order.

The expected value of the output when the rest of the uncertain variables are defined is given as:

$$E_{x_i}(Y|\tilde{x}_i = \tilde{x}_i^*), \tag{24}$$

where $\tilde{x}_i$ is the vector x without the parameter x_i. Since the constant $\tilde{x}_i^*$ can take values which span a domain, the variance of the conditional mean is calculated as:

$$V_{\tilde{x}_i}(E_{x_i}(Y|\tilde{x}_i = \tilde{x}_i^*)). \tag{25}$$

which has been shown to be the sum of the impact of all the terms excluding x_i (Saltelli et al., 2006), and consequently, the total effect is defined as:

$$S_{x_i}^T = 1 - V_{\tilde{x}_i}(E_{x_i}(Y|\tilde{x}_i = \tilde{x}_i^*)). \tag{26}$$

This term is called the *total effect* of x_i on Y since it includes all terms in the development of any order that do not include x_i.

Using the *law of total variance*:

$$V(Y) = V(E(Y|\tilde{x}_i)) + E(V(Y|\tilde{x}_i)), \tag{27}$$

the *total effect* of the parameter x_i can also be determined by evaluating:

$$S_{x_i}^T = E_{\tilde{x}_i}(V_{x_i}(Y|\tilde{x}_i = \tilde{x}_i^*)). \tag{28}$$

3.6. Computation

A major challenge in computing the metrics is the efficient computation of various expectation integrals. Conventionally, Monte Carlo (MC) methods are used for this purpose. While MC methods generally suffer from slow convergence rates, the common sampling strategies used to alleviate this problem (e.g., Markov Chain MC) cannot be parallelized effectively. An alternative to random sampling is a quadrature scheme, such as the popular Gaussian quadrature, which involves carefully choosing deterministic points to reproduce exactly the integrals for polynomials, i.e., moments of the density function. Gaussian quadrature

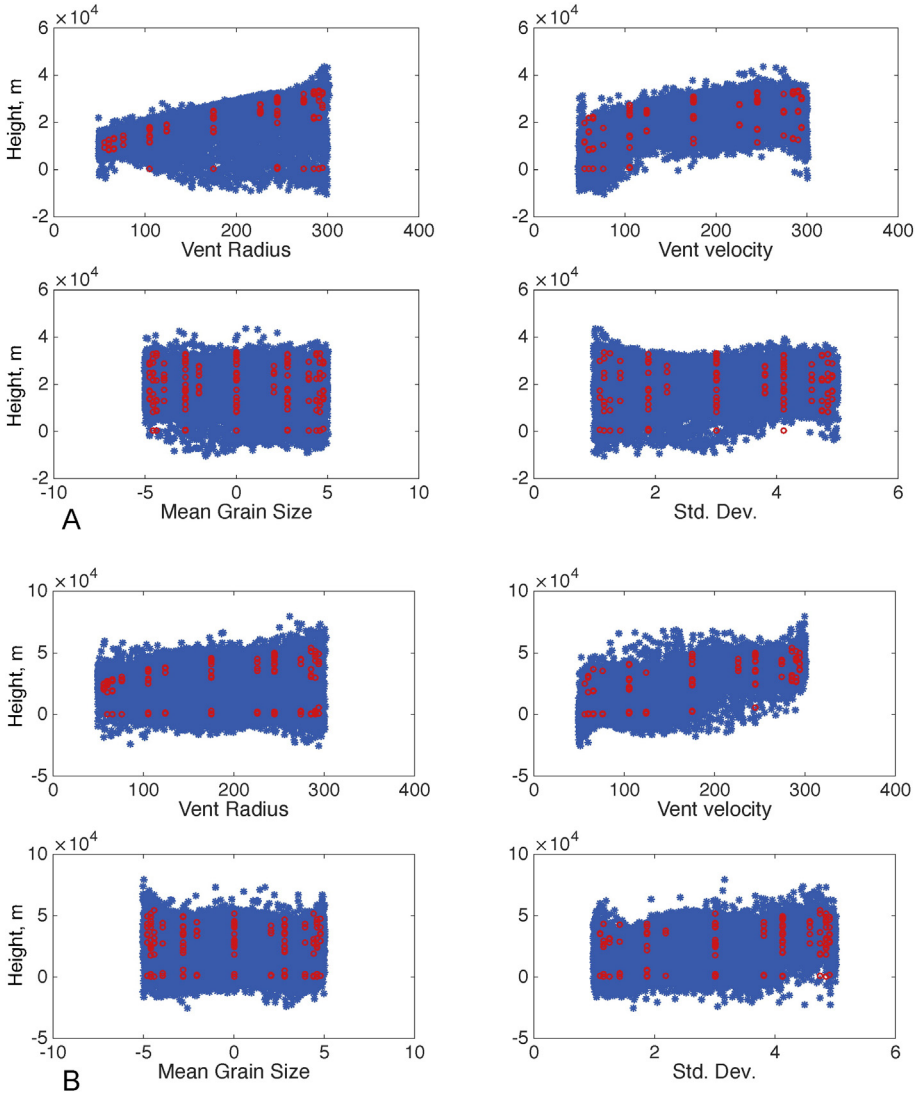

Fig. 4. H_T as a function of source parameters. A) $\alpha = 0.1890$, $\beta = 0.1170$, $w = 27.9 m/s$ (high entrainment and wind speed). B) $\alpha = 0.0606$, $\beta = 0.1170$, $w = 2.12$ m/s (low entrainment and wind speed). Blue stars, individual runs; red circles, mean for all runs at fixed value of indicated parameter (x-axis).

Please cite this article as: Pouget, S., et al., Sensitivity analysis of a one-dimensional model of a volcanic plume with particle fallout and collapse behavior, J. Volcanol. Geotherm. Res. (2016), http://dx.doi.org/10.1016/j.jvolgeores.2016.02.018

schemes exactly reproduce the integral of a polynomial of degree $2M-1$ with M^m points in a m-dimension space. The sparse-grid quadrature schemes, and in particular Smolyak quadrature, select a subset of the tensor product of the one-dimensional quadrature points using a recursive algorithm as outlined in (Gerstner and Griebel, 1998). Thus the resulting scheme has fewer points than the equivalent Gaussian quadrature rule, but at the cost of introducing negative weights (Gerstner and Griebel, 1998). Fortunately, the Gaussian quadrature rule is not minimal for $m \geq 2$, and there exist quadrature rules requiring fewer points in high dimensions (Stroud and Secrest, 1966). As volcanic plume models, of which the one-dimensional ones are currently inexpensive to evaluate by design, become more expensive, the move to quadrature schemes becomes increasingly important.

There is no guarantee that collocation or quadrature methods will better capture the moments of an output variable, Y. Collocation and quadrature schemes are based upon the premises that one can increase the accuracy of moment calculations in Y-space by capturing more moments in X-space, for example, let us assume that $Y=f(X)$, hence $E[Y]=E[f(X)]$. If one does the Taylor series expansion of $f(X)$, then $E[Y]$ is a function of the moments of X, hence capturing higher order moments of X leads to more accuracy in capturing moments of Y.

In this work, a non-product quadrature rule known as the Conjugate Unscented Transformation (CUT) (Adurthi et al., 2013a) has been exploited to compute the various expectation integrals. Rather than using tensor products as in Gauss quadrature, the CUT approach judiciously selects special structures to extract symmetric quadrature points constrained to lie on specially defined axes. The CUT algorithm has been benchmarked in earlier papers against other approaches for convergence of the moments (Adurthi et al., 2013a, 2013b, 2012; Adurthi and Singla, 2015). Madankan et al. (2014) specifically tested convergence for the present plume model coupled to the ash dispersion model, PUFF.

These specially designed axes are derivatives of the *principal axes*, σ, defined as the n orthogonal axes, centered at the origin, that are orthogonal to the pdfs of the input variables (Fig. 1). In an $n-$dimensional Cartesian space, the m *conjugate axis* with $m \leq n$, are defined as the directions that are constructed from all the combinations, including the sign permutations, of the set of principal axes, taken m at a time. The set of m conjugate axes, c^m, determine points, c_i^m:

$$c_i^m \in \{(\pm\sigma_{N_1} \pm \sigma_{N_2} \ldots \pm \sigma_{N_m}) | \{N_1, N_2, \ldots, N_m\} \subset \mathcal{D}\}\ i = 1, 2, \cdots, 2^m \binom{n}{m}.$$

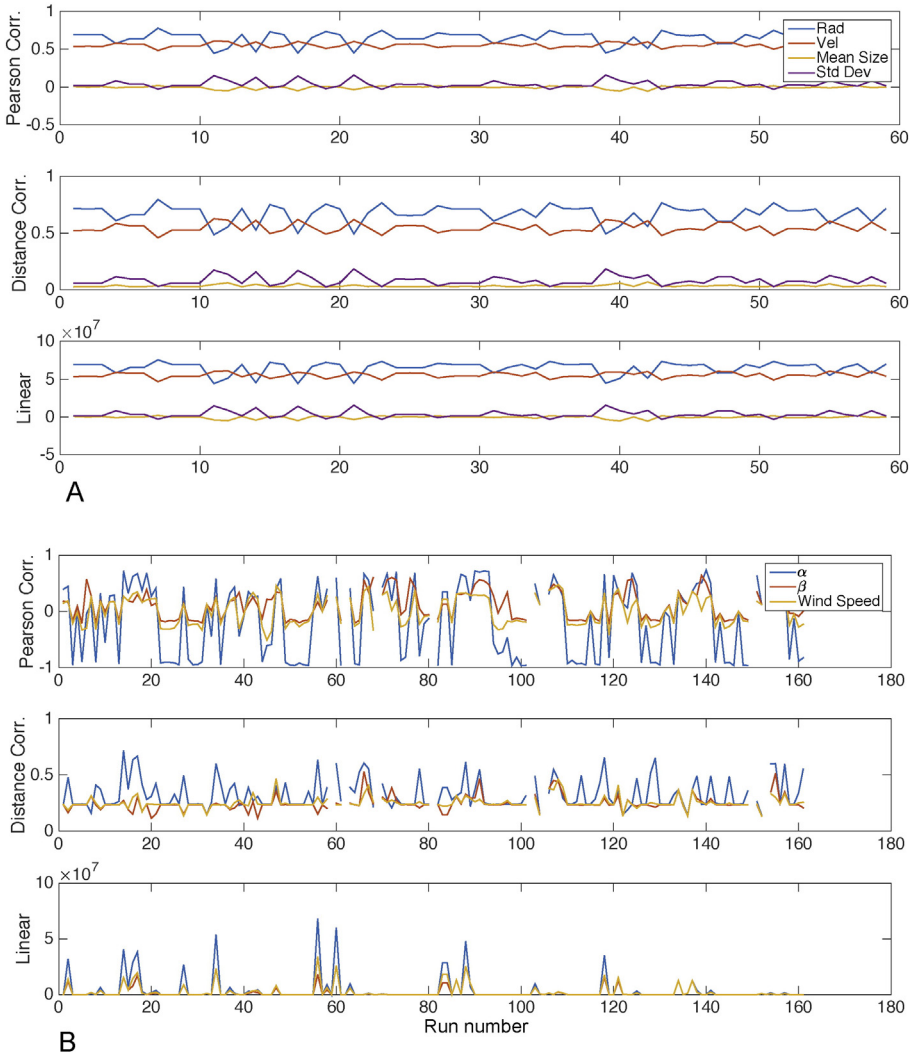

Fig. 5. Different sensitivity metrics for particle flux, $\dot{m}_p|_{H_B}$. Each run number refers to computational run using different CUT point (set of values of variables being tested for sensitivity). A) Sensitivity as a function of model parameters. B) Sensitivity as a function of source conditions. For column collapse, sensitivity metrics cannot be computed for $\dot{m}|_{H_T}$ because no ash output.

Please cite this article as: Pouget, S., et al., Sensitivity analysis of a one-dimensional model of a volcanic plume with particle fallout and collapse behavior, J. Volcanol. Geotherm. Res. (2016), http://dx.doi.org/10.1016/j.jvolgeores.2016.02.018

In $n-$dimensional Cartesian space, the *m-scaled conjugate axes* are defined as the set of directions constructed from all combinations, including sign permutations, of the set of principal axes such that in every combination exactly one principal axis is scaled by a parameter, h. The set of m scaled conjugate axes, s^m, determine points, s_i^m:

$$s_i^m \in \{(\pm h\sigma_{N_1} \pm \sigma_{N_2} \ldots \pm \sigma_{N_m}) | \{N_1, N_2, \ldots, N_m\} \subset \mathcal{D}\}\ i = 1, 2, \ldots, n2^m \binom{n}{m}.$$

Fig. 1a shows a perspective view of the first octant of the Cartesian space for a $3-$dimensional case. It should be mentioned that all eight octants in the $3-$dimensional case are symmetrical.

For each cubature point, two unknown variables, a weight w_i and a scaling parameter r_i are assigned. The moment constraint equations for the desired order are derived in terms of unknown variables r_i and w_i. Because of the symmetries of cubature points, the odd-order moment constraint equations are automatically satisfied, so the w_i and r_i are found by solving just the even-order equations. Different sets of cubature points can be found, depending on m and the order of the moment constraint equations.

These new sets of so-called sigma points are guaranteed to exactly evaluate expectation integrals involving polynomial functions with significantly fewer points. More details about the CUT methodology and its comparison with conventional quadrature rules can be found in (Adurthi et al., 2013a,b, 2012; Adurthi and Singla, 2015).

The CUT quadrature approach uses a small number of points, relative to Gauss quadrature, to compute an integral with the same accuracy. Fig. 2 represents the number of quadrature points required, for 8th order accuracy, by different quadrature schemes (CUT, Gauss–Legendre, Clenshaw–Curtis and Sparse Grid), for a uniform random variable, as a function of the dimensionality of the random variable. From the figure, it is clear that the growth in the number of quadrature points with dimension is much smaller for the CUT method, especially compared to the Gauss–Legendre and Clenshaw–Curtis approaches. The CUT method requires fewer than half the number of quadrature points for the sparse-grid Smolyak approach. As one specific example, 161 CUT quadrature points are required to satisfy 8th-order moments in 4-dimensional space, but 6561 points are required for Clenshaw–Curtis quadrature, 625 for Gauss–Legendre quadrature, and 385 for sparse-grid quadrature.

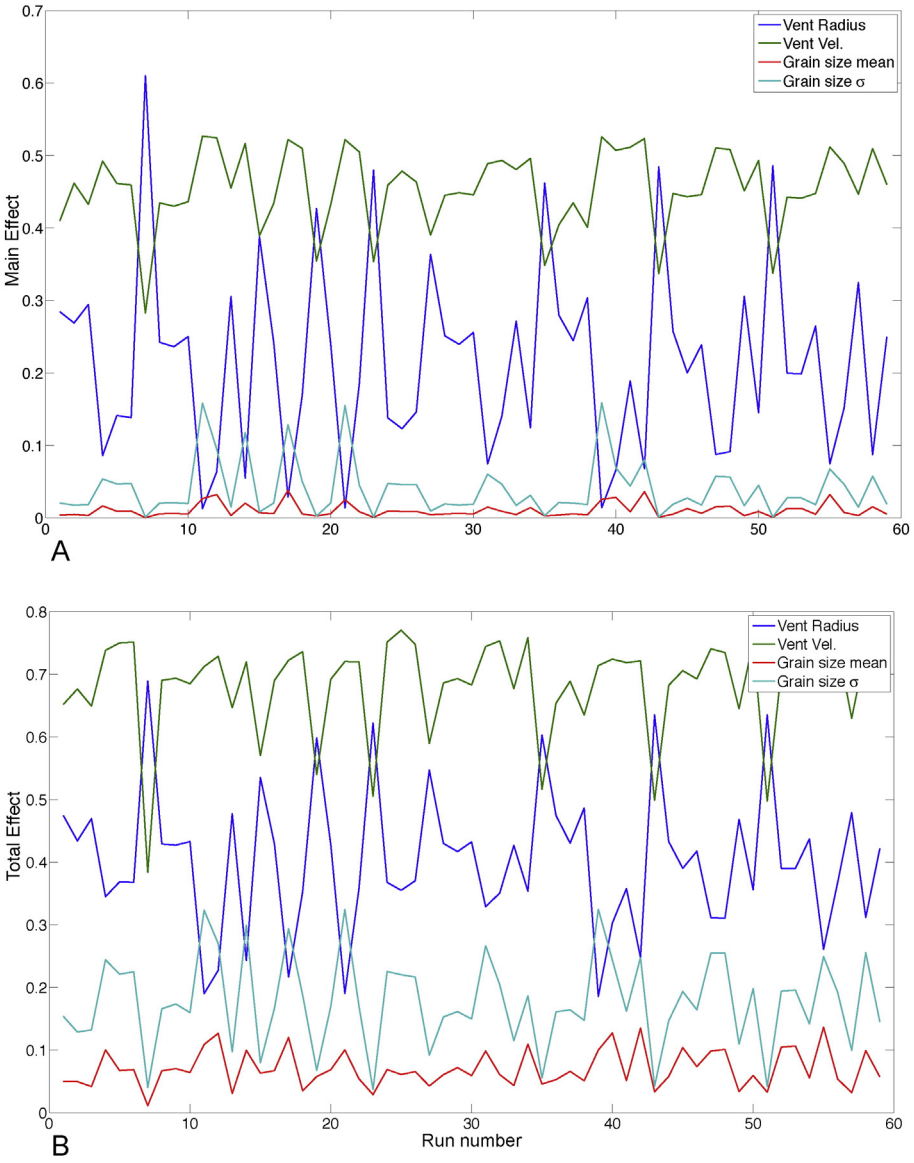

Fig. 6. Global sensitivity metrics for source conditions. Each run number refers to computational run using different CUT point (set of values of variables being tested for sensitivity). A) Main effect. B) Total effect.

Please cite this article as: Pouget, S., et al., Sensitivity analysis of a one-dimensional model of a volcanic plume with particle fallout and collapse behavior, J. Volcanol. Geotherm. Res. (2016), http://dx.doi.org/10.1016/j.jvolgeores.2016.02.018

While the computation of the Pearson correlation coefficient, the linear correlation coefficient and the global sensitivity measures can be carried out with the CUT quadrature points (as they need only the information about the statistical moments), the computation of the distance correlation metric requires statistical samples of input and output variables, i.e., X and Y. A 5^{th}-order polynomial surrogate for the plume model is developed to derive a large number of Monte Carlo samples for the output variables, corresponding to various MC samples of input variables. The surrogate is thus an analytic, polynomial expression that substitutes for the numerical integration of the plume model to describe the values of specified output variables given ranges of potential values (uncertainty) in a set of input variables. The model output, Y, can be written as a linear combination of polynomial basis functions, $\phi_k(\boldsymbol{\xi})$, orthogonal to the density function for the input variable, $\boldsymbol{\xi}$. These can be computed by Gram-Schmidt orthogonalization, and span the space of the random input variables $\boldsymbol{\xi} = [X_1, \ldots X_m]^T$:

$$Y(\xi) = \sum_{k=0}^{N} Yk\phi k(\xi) \quad Yk = \frac{E[Y(\xi)\phi_k(\xi)]}{E[\phi_k(\xi)\phi_k(\xi)]}, j = 1, 2, \ldots, m. \tag{29}$$

These expectation integrals can once again be computed with the help of CUT methodology. In Bursik et al. (2012); Madankan et al. (2014), the CUT methodology, in conjunction with a 5th-order polynomial surrogate model, is successfully applied to compute a probabilistic, spatio-temporal estimate of ash presence during the April, 2010 eruption of Eyjafjallajökull, Iceland.

4. Results and discussion

Given the uncertain ranges of various parameters (Table 1), 161 8th-order CUT points were generated for the four boundary conditions, and 59 8th-order CUT points were generated for the three model parameters. For each set of variables, the sensitivity metrics illustrating the correlation between H_T or $\dot{m}|_{H_T}$ and the inputs were computed directly from the CUT points. The only exception is the distance correlation coefficient, which is computed with the help of 50,000 MC runs generated from a 5^{th}-order polynomial surrogate model, the coefficients of which are generated from the CUT points.

Fig. 3A shows the plot of the sensitivity metrics for H_T as a function of the 59 CUT runs of the plume model, each run with different, but fixed values of the model parameters, while the source conditions are varied. No matter the value of the model parameters, all metrics concur in the parameters most and least correlated to plume rise height, H_T. Irrespective of the value of the model parameters, the ash particle mean size is the variable least correlated to H_T, while the Pearson coefficient indicates H_T is most highly correlated to the source velocity, followed by vent radius. This is in accordance with the physics of the model, as the product of the source velocity and squared vent radius represents the total mass flux from the vent, which controls H_T. The more consistent dependence of rise height on velocity than on radius in the Pearson and Linear coefficients results from the fact that for a given fixed velocity, an increase in radius can result in column collapse, i.e., lowering rather than raising of H_T Sparks et al. (1997), while at a fixed vent radius, an increase in velocity never results in collapse, i.e., H_T is more nearly linearly dependent on source velocity. The more complex functional dependence on vent radius is reflected in the Distance coefficient, which almost always has a higher value for vent radius than for velocity.

Fig. 3B shows the plot of the sensitivity metrics corresponding to H_T and the three model parameters, as a function of 161 different CUT runs for different, but fixed values of the source conditions. Each sample thus represents the sensitivity of the model rise height to the given plume parameter. The entrainment parameter α correlates most highly to H_T, while β and wind speed are equally important. The effect of β is almost the same as the effect of wind speed, through the relation expressed in Eq. (3). With a few exceptions, due perhaps to unexplored nonlinearity, the Pearson and Linear coefficients display a negative dependence for all model parameters, while the Distance coefficient shows a greater sensitivity to α than to β and wind speed. The negative dependence results from the decrease in the neutral buoyancy level (H_B) with increasing entrainment – the plume is driven towards the atmospheric density more rapidly. The Distance coefficient shows that this dependence of H_B is more correlated with α, rather than β and wind speed, due to other effects on plume dynamics. For example, wind speed directly affects momentum flux (Eqs. (7), (8)), making additional accelerations possible as H_B is approached.

Fig. 4A and B show the outputs of the emulator runs for specific values of model parameters. These are emulator runs, not simulations (actual runs of the numerical model), so it is possible for negative heights to be generated. Nevertheless, the moments of the distributions of the runs are accurate (Madankan et al., 2014; Adurthi and Singla, 2015). When the model parameters take on lower values (Fig. 4B), rise height increases due to slower atmospheric mixing and increase in H_B. Column collapse is more common with increased vent radius and decreased initial velocity, as expected. Rise height is not sensitive to particle size over the range of values investigated herein, as the range does not extend to coarser particle sizes associated with fountaining (Woods and Bursik, 1991).

Fig. 5A shows the sensitivity metrics corresponding to particle flux at the neutral buoyancy level, $\dot{m}_p|_{H_B}$, and four source conditions, as a function of 59 CUT runs on the model parameters. Similarly, Fig. 5B shows the sensitivity metrics corresponding to particle flux and three model parameters, as a function of the 161 CUT runs for the source conditions. Once again, in considering the uncertain ranges for the model parameters, the vent radius and source velocity are highly correlated to the particle flux. All three model parameters are almost equally and positively

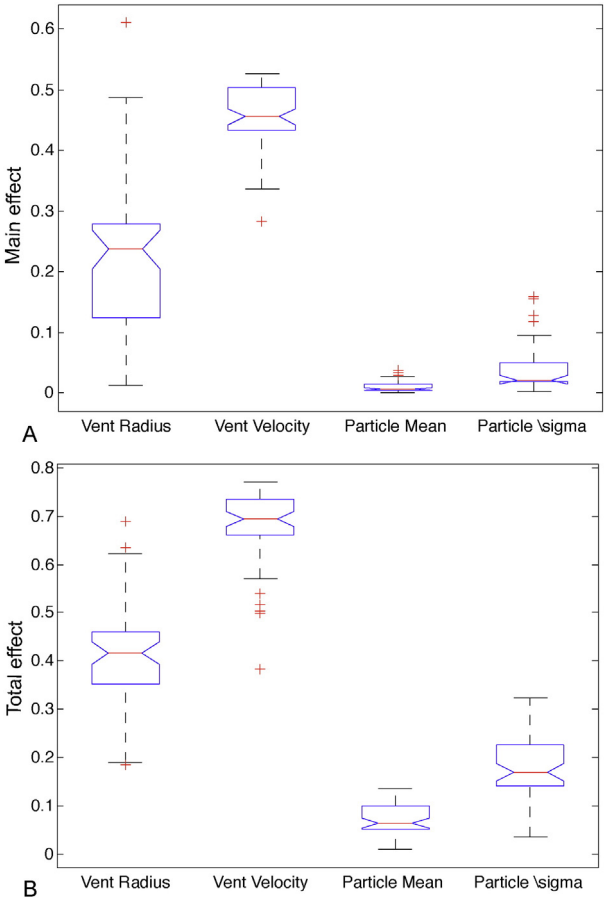

Fig. 7. Box and whisker plots for source conditions. A) Main effect. B) Total effect.

Please cite this article as: Pouget, S., et al., Sensitivity analysis of a one-dimensional model of a volcanic plume with particle fallout and collapse behavior, J. Volcanol. Geotherm. Res. (2016), http://dx.doi.org/10.1016/j.jvolgeores.2016.02.018

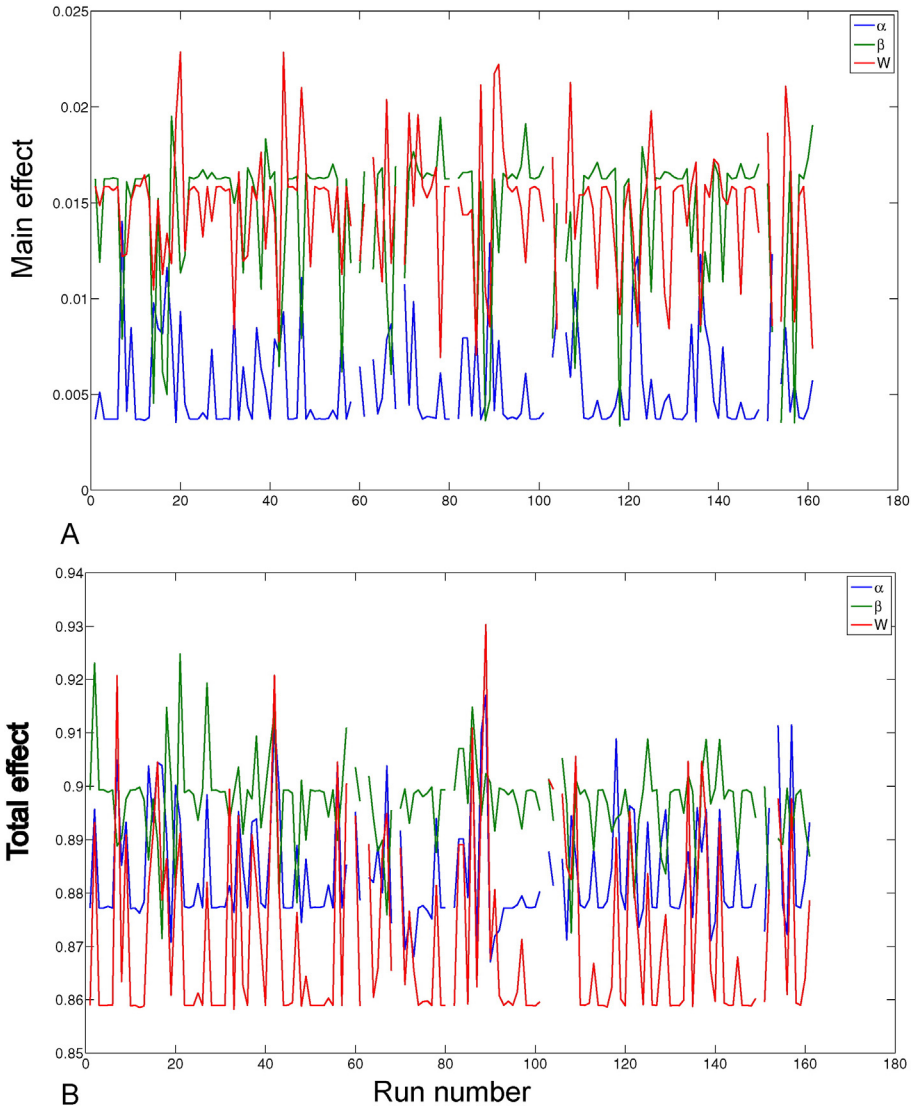

Fig. 8. Global sensitivity metrics for model parameters. Each run number refers to computational run using different CUT point (set of values of variables being tested for sensitivity).A) Main effect. B) Total effect.

correlated to the particle flux for most values of the eruption source conditions, but for some values, the Pearson coefficient shows high negative correlation for α. At these values, the Distance coefficient shows weaker correlation and the Linear coefficient suggests no correlation. For other values, the Distance coefficient shows a greater degree of correlation. At these values, the Pearson and Linear coefficients sometimes show a greater positive correlation. Exploration of such occasional model nonlinearities that cause these unusual relations for α are beyond the scope of the present work.

The global sensitivity measures confirm the relative importance of the source parameters on the primary output considered: plume height, H_T. Fig. 6A and B illustrate the variation of the relative importance of the four source parameters for the 59 CUT runs of model parameters. Fig. 7A and B are box and whisker charts which illustrate the spread of the Main and Total effect metrics for the 59 CUT runs. Box and whisker plots are used to display a statistical population without making any assumption of the distribution. The box part of the plot contains three horizontal lines. The middle corresponds to the median, the bottom and top lines correspond to the 25th and 75th percentiles, respectively. The whiskers represent the bounds of the data excluding data points considered as outliers, which are represented individually. The source velocity is shown to be the most important variable, with a small spread, indicating that irrespective of the region of the uncertain source parameter space sampled, its importance was consistent. The global measures confirm the complex functional relation between the vent radius and plume height, with a much greater spread in effect than source velocity. The effects of particle mean and standard deviation on output H_T are lower than source velocity or vent radius, with little variability, particularly, in the mean grain size.

The main effect and the total effect on H_T as a function of the uncertain inputs α, β and wind speed, are calculated for 161 runs that correspond to different realizations of the model parameter values. Across the set of volcanic model parameters, both the main effect (Fig. 8A) and the total effect (Fig. 8B) chart the characteristic that the contributions of all of the uncertain parameters are about the same. The box and whisker charts (Fig. 9A and B) illustrate the same assessment, i.e., the impact of the variables α, β and wind speed over their uncertain ranges is nearly the same. In contrast to the global sensitivity analysis for the volcanic source conditions, where the initial velocity and vent radius were clearly the dominant variables, accounting for a majority of the variability in the output, there is little to distinguish the overall impact of α, β and wind speed on the output. The center of the distribution of values

Please cite this article as: Pouget, S., et al., Sensitivity analysis of a one-dimensional model of a volcanic plume with particle fallout and collapse behavior, J. Volcanol. Geotherm. Res. (2016), http://dx.doi.org/10.1016/j.jvolgeores.2016.02.018

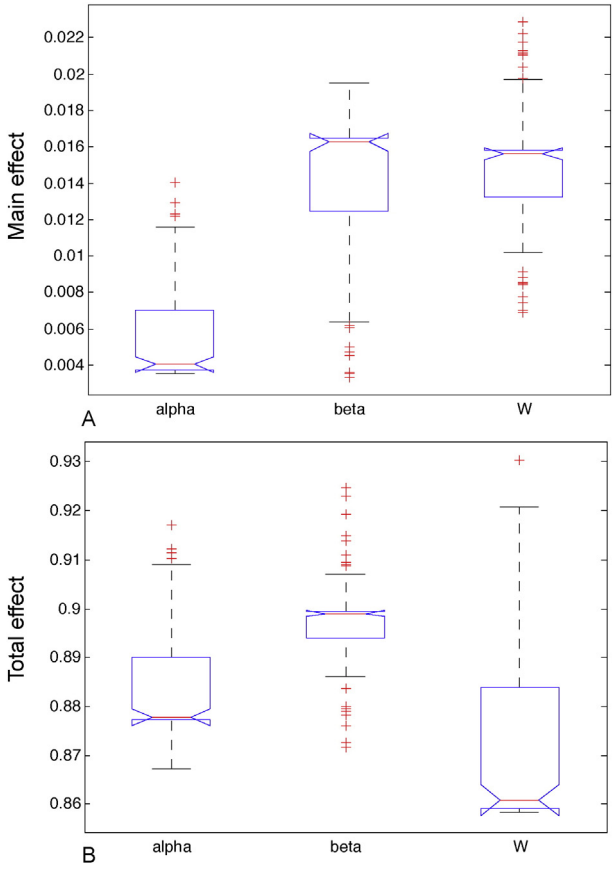

Fig. 9. Box and whisker plots for model parameters. A) Main effect. B) Total effect.

for the Main effect is noticeably lower for α than for the other two parameters, but the outliers and 25 — 75% range overlap considerably.

5. Conclusions

In the present contribution, we have investigated the effects of the main source conditions (vent radius, initial velocity and grain size distribution) on rise height and particle mass flux at H_B, into the umbrella cloud of a volcanic plume. For the plume model investigated herein, vent radius and initial speed have a much more profound effect on both outputs than does total grain size distribution. Plume rise height and particle mass flux at H_B are sensitive to the entrainment parameters, α and β, but these values are not of greater importance than correctly characterizing the wind speed. This suggests that while efforts to better characterize entrainment parameters through laboratory experiments are important, similar effort should be made to collect accurate meteorological data near the site of the eruption.

Acknowledgments

This research was supported by NSF-IDR CMMI grant number 1131074 to E.B. Pitman, and by AFOSR grant number FA9550-11-1-0336 to A.K. Patra. All results and opinions expressed in the foregoing are those of the authors and do not reflect opinions of NSF or AFOSR. The paper was greatly improved by the comments of M. Woodhouse and an anonymous reviewer, whom we thank.

We dedicate this paper to our dear colleague, protegée and friend: Dr. Solène Pouget, who was the driving force for this sensitivity analysis, but whom we lost forever while working on this manuscript. Solène, you fought with grace and dignity. You lived a happy, compassionate and productive life and inspired everyone around you. Your legacy will live indefinitely through your excellent work.

References

Adurthi, N., Singla, P., Singh, T., 2012. Conjugate unscented transform and its application to filtering and stochastic integral calculation. Proceedings of the AIAA Guidance, Navigation, and Control Conference. http://dx.doi.org/10.2514/6.2012-4934.

Adurthi, N., Singla, P., Singh, T., 2013a. Optimal information collection for nonlinear systems: an application to multiple target tracking and localization. Proceedings of the American Control Conference. http://dx.doi.org/10.1109/ACC.2013.6580429.

Adurthi, N., Singla, P., Singh, T., 2013b. Conjugate unscented transform rules for uniform probability density functions. Proceedings of the American Control Conference. http://dx.doi.org/10.1109/ACC.2013.6580202.

Adurthi, N., Singla, P., 2015. Conjugate unscented transformation-based approach for accurate conjunction analysis. J. Guid. Control. Dyn. 38, 1642–1658. http://dx.doi.org/10.2514/1.G001027.

Bursik, M., 2001. Effect of wind on the rise height of volcanic plumes. Geophys. Res. Lett. 28 (18), 3621–3624.

Bursik, M., Jones, M., Carn, S., Dean, K., Patra, A., Pavolonis, M., et al., 2012. Estimation and propagation of volcanic source parameter uncertainty in an ash transport and dispersal model: application to the Eyjafjallajökull plume of 14–16 April 2010. Bull. Volcanol. 74 (10), 2321–2338.

Bursik, M.I., Carbonara, A.U., Zawicki, S.M., 2013. Puffin. https://vhub.org/resources/puffin.

Bursik, M.I., Kobs, S.E., Burns, A., Braitseva, O.A., Bazanova, L.I., Melekestsev, I.V., Kurbatov, A., Pieri, D.C., 2009. Volcanic plumes and wind: jetstream interaction examples and implications for air traffic. J. Volcanol. Geotherm. Res. 186, 60–67.

Chu-Agor, M.L., Muñoz-Carpena, R., Kiker, G., Emanuelsson, A., Linkov, I., 2011. Exploring vulnerability of coastal habitats to sea level rise through global sensitivity and uncertainty analyses. Environ. Model. Softw. 26, 593–604.

Degruyter, W., Bonadonna, C., 2012. Improving on mass flow rate estimates of volcanic eruptions. Geophys. Res. Lett. 39 (16).

Ernst, G.G.J., Carey, S.N., Sparks, R.S.J., Bursik, M.I., 1996. Sedimentation from turbulent jets and plumes. J. Geophys. Res. 101, 5575–5589.

Folch, A., Cavazzoni, C., Costa, A., Macedonio, G., 2008. An automatic procedure to forecast tephra fallout. J. Volcanol. Geotherm. Res. 177 (4), 767–777.

Gerstner, T., Griebel, M., 1998. Numer. Algorithm. 18, 209–232. http://dx.doi.org/10.1023/A:1019129717644.

Glaze, L.S., Baloga, S.M., 1996. Sensitivity of buoyant plume heights to ambient atmospheric conditions: implications for volcanic eruption columns. J. Geophys. Res. 101, 1529–1540.

Hewett, T.A., Fay, J.A., Hoult, D.P., 1971. Laboratory experiments of smokestack plumes in a stable atmosphere. Atmos. Environ. 5, 769–789.

Kaminski, E., Tait, S., 2005. Turbulent entrainment in jets with arbitrary buoyancy. J. Fluid Mech. 526, 361–376.

Madankan, R., Pouget, S., Singla, P., Bursik, M., Dehn, J., Jones, M., Patra, A., Pavolonis, M., Pitman, E., Singh, T., et al., 2014. Computation of probabilistic hazard maps and source parameter estimation for ash transport and dispersion. J. Comput. Phys. 271, 39–59.

Morton, B., Turner, J., Taylor, G., 1956. Gravitational turbulent convection from maintained and instantaneous sources. Proc. R. Soc. Lond. Ser. A234, 1–23.

Pappenberger, F., Beven, K.J., Ratto, M., Matgen, P., 2008. Multi-method global sensitivity analysis of flood inundation models. Adv. Water Resour. 31, 11–14.

Saltelli, A., Ratto, M., Tarantola, S., Camplongo, F., 2006. Sensitivity analysis practices: strategies for model-based inference. Reliab. Eng. Syst. Saf. 91, 1109–1125.

Saltelli, A., Tarantola, S., Campolong, F., Ratto, M., 2004. Sensitivity Analysis in Practice: A Guide to Assessing Scientific Models. Halsted Press, New York, NY.

Scollo, S., Folch, A., Costa, A., 2008. A parametric and comparative study of different tephra fallout models. J. Volcanol. Geotherm. Res. 176 (2), 199–211.

Spanos, P., 1981. Stochastic linearization in structural dynamics. Appl. Mech. Rev. 34 (1), 1–8.

Sparks, R.S.J., Bursik, M.I., Carey, S.N., Gilbert, J.S., Glaze, L.S., Sigurdsson, H., Woods, A.W., 1997. Volcanic Plumes. J. Wiley and Sons, Chichester, UK (574 pp.).

Stefanescu, E.R., Patra, A.K., Bursik, M.I., Madankan, R., Pouget, S., Jones, M., Dehn, J., 2014. Temporal, probabilistic mapping of ash clouds using wind field stochastic variability and uncertain eruption source parameters: example of the 14 April 2010 Eyjafjallajökull eruption. J. Adv. Model. Earth Syst. 6 (4), 1173–1184.

Stroud, A.H., Secrest, D., 1966. Gaussian Quadrature Formulas. Prentice Hall, Englewood Cliffs, NJ.

Székely, G.J., Rizzo, M.L., Bakirov, N.K., 2007. Measuring and testing dependence by correlation of distances. Ann. Stat. 35 (6), 2769–2794.

van Griensven, A., Meixner, T., Grunwald, S., Bishop, T., Diluzio, M., Srinivasan, R., 2006. A global sensitivity analysis tool for the parameters of multivariable catchment models. J. Hydrol. 324, 10–23.

Wang, H., Law, A.W.-K., 2002. Second-order integral model for a round turbulent buoyant jet. J. Fluid Mech. 459, 397–428.

Woodhouse, M.J., Hogg, A.J., Phillips, J.C., Rougier, J.C., 2015. Uncertainty analysis of a model of wind-blown volcanic plumes. Bull. Volcanol. 77 (10), 1–28.

Woods, A.W., Bursik, M.I., 1991. Particle fallout, thermal disequilibrium and volcanic plumes. Bull. Volcanol. 53 (7), 559–570.

Woods, A.W., Bower, S.M., 1995. The decompression of volcanic jets in a crater during explosive volcanic eruptions. Earth Planet. Sci. Lett. 131, 189–205.

Wright, S., 1984. Buoyant jets in density-stratified crossflow. J. Hydraul. Eng. 110, 643–656.

Please cite this article as: Pouget, S., et al., Sensitivity analysis of a one-dimensional model of a volcanic plume with particle fallout and collapse behavior, J. Volcanol. Geotherm. Res. (2016), http://dx.doi.org/10.1016/j.jvolgeores.2016.02.018